

Visualization and Analysis of Nanostructure Evolution During the Crystallization and Melting Processes of Oriented Poly (ethylene) from Time-Resolved 2D SAXS and WAXS Data

Norbert Stribeck¹, Rüdiger Bayer², Armando Almendarez Camarillo¹, Peter Bösecke³ and Rainer Gehrke⁴

¹Universität Hamburg, Institut TMC, Bundesstr. 45, 20146 Hamburg, Germany

²Universität GH Kassel, Institut f. Werkstofftechnik, 34125 Kassel, Germany

³ESRF Grenoble, France

⁴HASYLAB at DESY, 22603 Hamburg, Germany

ABSTRACT

The structure transfer between an oriented polymer melt and the solid semicrystalline state is central for the optimization of materials properties but still not sufficiently explored. For the first time we present real space image series of the nanostructure evolution generated by Fourier inversion from high-resolution time-resolved two-dimensional small-angle X-ray scattering (SAXS) images and related wide-angle X-ray scattering (WAXS) patterns recorded at the ESRF, Grenoble (cycle time 7 s, exposure 0.1 s – 3 s). From the continuous movies detailed insight into the structure transfer mechanisms is obtained.

Quantitative data analysis has already been performed on similar data recorded at HASYLAB, Hamburg (cycle and exposure time 120 s). The results show that ordered placement of crystallites is the exception. There is no lattice. A random car parking process¹ is governing the formation of lamellae “stacks”. The observed long period is not related to a regular repeat distance, but only to the layer thickness and the Rényi limit.² Under these premises not distortions of some lattice ought to be studied, but order generating mechanisms should be searched for in the dominant random process. Two such processes found in our data have been identified.

The high-resolution data from the ESRF show that crystallization is induced by the oriented network of entangled chains. The cool melt is not homogeneous. Instead, it contains entanglement-rich domains of varying size and orientation. Nucleation appears to be induced at the ends of these “entanglement strands”. Continuous lateral growth of primary lamellae is observed from the active sites (no blocks). If both ends of a strand are fertile, the corresponding lamellae are separated by the height of the entanglement strand. Growth of lamellae thickness (outward from the strand end) is observed in the next period. Only in the last period block-shaped crystals (frustrated lamellae) show up. They form strong correlations (short-range lattice) with the primary lamellae and with each other (Strobl¹ block structure) and, in the end, dominate the nanostructure and the features of the scattering pattern.

EXPERIMENTAL

Material. High-pressure injection molded rods from Lupolen 6021 D (BASF) were molten and re-crystallized in the synchrotron beam of beam line ID02 at the ESRF in Grenoble. More information on the material is in a previous paper.³

Melting and Crystallization. At a rate of 2°C/min the samples were molten in an oven up to a melt-annealing temperature of 140°C

and kept there for ca. 2 min until the SAXS and the WAXS appeared to be vanished. Then the samples were quenched to a crystallization temperature (130°C, 126°C, 120°C). Isothermal crystallization was studied in the following 30 min. Finally the samples were either quenched (20°C/min) or cooled (2°C/min) to ambient temperature.

Data Recording at ESRF. Data were recorded using two two-dimensional detectors (one detector for the collection of ultra small-angle X-ray scattering patterns in a distance of 10 m to the sample, and an offset wide-angle X-ray scattering detector close to the sample). In the critical regions of the temperature profile the cycle time was set to 7 s. This setup facilitates in-situ optimization of the exposure time.

Data Recording at HASYLAB. Results of similar experiments obtained with only one old USAXS detector at beam line BW4 (HASYLAB, Hamburg) have already been submitted for publication.⁴⁻⁶ At HASYLAB several compromises had to be accepted because of the old detector and the low brilliance of the beam line. Cycle time was 2 min, and detector sensitivity was manually changed during the experiment.

DATA ANALYSIS

2D SAXS patterns with fiber symmetry are transformed into multidimensional chord distribution function (CDF)⁷, which is the correlation function of the nanodomain surfaces in real space. For quantitative analysis of the crystallite stacking we extract from the CDFs interface distribution functions (IDFs)⁸ and analyze these curves by models based on domain thickness distributions and their arrangement.

Computer programs are developed for pv-wave⁹ under Linux. After adaption of the programs to the experimental setup and a frame-by-frame control of image alignment, the CDF is computed automatically. Trying to cope with the flood of data by spot testing led to false conclusions. So for every snapshot we mount images of SAXS, WAXS and the CDF (from two different view points) in a composite picture (programs: PoVRay, ImageMagick). This series is finally transformed (transcode) into avi-movies of about 3 min length which finally can be replayed (mplayer). Thus the mechanisms of crystallization are revealed.

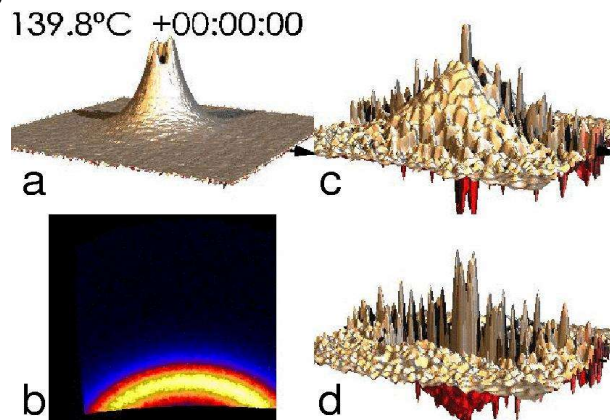


Figure 1. The oriented melt. (a) SAXS, (b) WAXS, (c) CDF, domain face up (d) CDF, lattice face up. The CDF shows a region $|r_{12}, r_3| < 300$ nm (cylindrical coordinates in real space). Arrows: meridian. The WAXS meridian is almost vertical.

RESULTS

Early Stages of Crystallization. Figure 1 shows one of the images of one of the movies. It describes the nanostructure of the oriented melt. The SAXS (a) appears diffuse. The WAXS (b) shows only an amorphous halo. In the CDF (c, d), we observe the staggered structure of various rows extending along the fiber direction (meridian).

The movie exhibits their volatility. The peaks on the domain face (c) are resulting from correlations between opposite surfaces of domains (i.e. from the beginning of a nucleus to its end or to the end of a neighbor). The peaks on the negative face (d) of the CDF are related to conjunctions (i.e. from the beginning of a nucleus to the beginning of a neighbor).

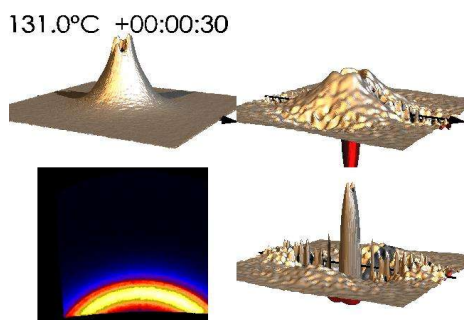


Figure 2. Nanostructure of the oriented melt. Crystallization is about to start (30 s after the start of quenching).

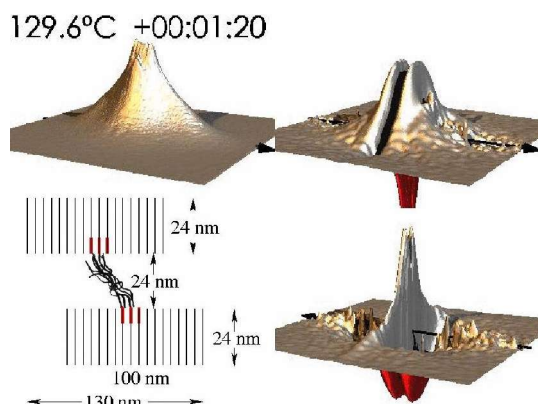


Figure 3. Lamellae have extended from the tips of the entanglement strands in lateral direction.

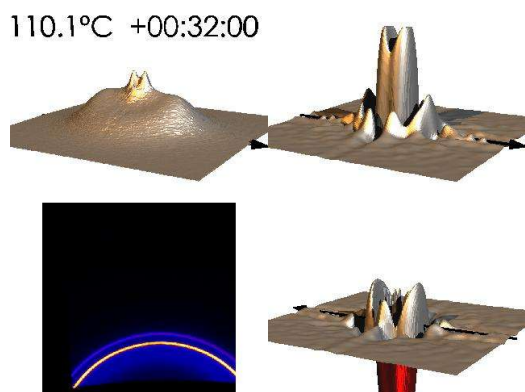


Figure 4. Blocks have populated the remnant amorphous zones and formed short-range correlated ensembles in which the primary lamellae are incorporated. The blocks show no preferred orientation.

Related to the row structure we observe a pyramid-shaped correlation made from opposite surfaces of some kind of domain (our interpretation: entanglement strand) that is extending out into space and has its maximum at the origin of the coordinate system. Here the most probable entanglement strand is a single entanglement.

Just as formation of lamellae starts (Figure 2), the most probable entanglement strand is extending 24 nm in fiber direction and 30 nm in perpendicular direction. Between the corresponding peaks, on the meridian, the first lamellae become visible (Figure 3). There is some WAXS orientation, but it is low.

In the sequel we observe growth of lamellae thickness (no graph shown here) – away from the nucleating entanglement strand. It goes along with the improvement of WAXS orientation. Finally the generation of unoriented, crystalline blocks is observed (Figure 4). These secondary crystallites are small, unoriented but well-positioned: They undergo strong correlations among each other and with the primary lamellae.

Placement of Crystallites Along the Fiber Axis. The initial placement of layers along the fiber axis is more or less random and resembles the random car parking process.¹ By analysis of the IDFs from the primary crystallization regime only a weak ordering process is found (Figure 5a).

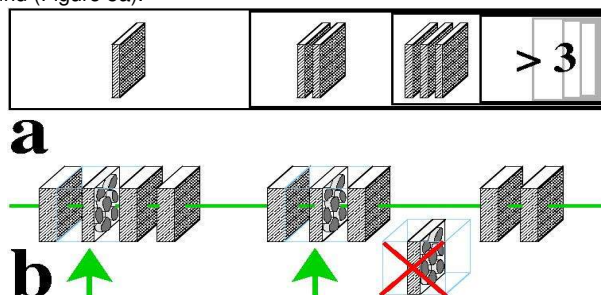


Figure 5. The order generating processes extracted from model fits of the SAXS. (a) weak process predominant during the primary crystallization in the beginning of the isothermal phase. (b) strong process predominant during secondary crystallization.

One coupling constant c describes the weak process. Let $c=0.4$ (Figure 5a). Then 40% of the lamellae are solos. The rest is correlated. From this rest, again 40% are organized in duos. The rest is organized in trios or higher correlation The strong process found by analysis of the HASYLAB data (Figure 5b) describes nothing but the strong tendency of the secondary blocks to undergo correlations, which is clearly shown in the videos of the ESRF measurements. In order to fit the HASYLAB data novel models for lamellae arrangement had to be developed, because the crystallization mechanism is inducing a special kind of correlation: The thick primary lamellae are more or less uncorrelated, whereas the small crystallites show a considerable correlation – but only with their closest neighbors.

ACKNOWLEDGEMENTS

We thank the European Synchrotron Radiation Facility, Grenoble, for beam time granted in the frame of project SC1396. The support of HASYLAB, Hamburg, project II-01-041, is gratefully acknowledged.

REFERENCES

1. Evans, J.W. *Rev. Mod. Phys.* **1993**, 65(4), 1281.
2. Rényi, A. *Sel. Transl. Math. Stat. Prob.* **1963**, 4(1), 203.
3. Stribeck, N.; Bayer, R.; v. Krosigk, G.; Gehrke, R. *Polymer* **2002**, 43(13), 3779.
4. Stribeck, N.; Almendarez Camarillo, A.; Cunis, S.; Bayer, R.K.; Gehrke, R. *Macromol. Chem. Phys.* **2004**, submitted
5. Stribeck, N. *Macromol. Chem. Phys.* **2004**, submitted
6. Stribeck, N.; Almendarez Camarillo, A.; Bayer, R.K. *Macromol. Chem. Phys.* **2004**, submitted.
7. Stribeck, N *J. Appl. Cryst.* **2001**, 34(4), 496.
8. Ruland, W. *Colloid Polym. Sci.* **1977**, 255(5), 417.
9. pv-wave Version 7.5 **2001**, Visual Numerics Inc., Boulder, CO.